JOURNAL OF MATERIALS SCIENCE 32 (1997) 4917–4923

Gamma prime (γ') precipitating and ageing behaviours in two newly developed nickel-base superalloys

H. T. KIM, S. S. CHUN
Department of Materials Science and Engineering, Korea Advanced Institute of Science and Technology, Taejon, Korea

X. X. YAO, Y. FANG
Department of Materials Science, Shanghai Jiao Tong University, Shanghai 200030, People's Republic of China

J. CHOI
Division of Metals, Korea Institute of Science and Technology, P.O. Box 131, Cheongryang, Seoul, Korea

Two cast nickel-base superalloys with superior creep rupture lives at high temperatures and high stresses were developed. In the present study, the microstructural characteristics of γ'-precipitates and the hardening behaviour were studied by electron microscopy and micro-hardness testing. The alloys were solution-treated at 1553 K for 2 h and air-cooled followed by step ageing heat treatments. Ageing up to 300 h at 1143, 1223 and 1293 K was carried out to examine the effects of ageing temperature and ageing time on the growth of γ'-precipitates. The growth kinetics of γ'-precipitates was analysed. The experimental evidence reveals that the morphology of γ' does not change in shape during heat treatments. The γ' is usually cubic in both Alloy B and Alloy C. Growth of γ' precipitates proceeds by Ostwald ripening controlled by volume diffusion of solute atoms despite the high volume fraction of γ' and complex compositions in these two alloys. The activation energies for the growth are evaluated as 272 and 277 kJ mol^{-1} for Alloy B and Alloy C, respectively, which correlate well to coarsening of γ' in other commercial and developed superalloys. The hardness increases to a peak value at about 20 to 60 h for Alloy B and at about 10 to 20 h for Alloy C during ageing. The hardness of the alloys hardly decreases and still maintains a high value at high temperatures after passing the hardness peak.

1. Introduction

Over the past decades, significant advances have been made in the development of new superalloys which are capable of operating at high service temperatures, thus enabling higher engine efficiencies to be realized. In order to function satisfactorily in more severe environments, superalloys must possess properties such as outstanding high temperature strength, creep and fatigue resistance, excellent ductility, good impact resistance and adequate resistance to hot corrosion.

Cast nickel-base superalloys are typically composed of high volume fractions of γ'-phase coherently precipitated in a face-centred cubic (fcc) matrix, together with eutectic phases and one or more carbide phases. The desired properties and resistance to microstructural changes at high temperatures in these alloys are obtained by all phases with suitable structure, shape, size and distribution. It is widely recognized nowadays that coarse-grained with serrated grain boundaries, homogeneous compositions with uniform cubic γ–γ' microstructures and small discrete phases at grain boundaries are typical microstructural features in modern advanced nickel-base cast superalloys. Among all the microstructural factors, the γ' precipitate morphology plays an important role in influencing the properties of nickel-base superalloys [1]. Therefore, one subject which is important to the development of new types of superalloy is how to produce the desirable γ' precipitate morphology.

In the present study, two newly developed Ni-base cast superalloys with higher strength and longer creep rupture lives than advanced conventional cast Ni-base superalloys Mar-M247 and TM-321 were chosen as the experimental materials [2, 3]. The age hardening behaviour and microstructural characteristics of these two alloys were investigated by hardness testing and scanning electron microscopy (SEM) and transmission electron microscopy (TEM). The growth kinetics of γ' precipitates is discussed.

0022–2461

TABLE I The chemical compositions of two developed alloys (wt %, balance = Ni)

Alloy	Cr	W	Mo	Al	Ti	Nb	Co	Ta	Hf	Zr	B	C
B	10.4	8.02	1.75	4.35	1.00	1.07	8.29	3.23	0.80	0.057	0.022	0.14
C	8.48	9.68	1.76	4.52	0.95	1.02	9.55	5.16	0.07	0.082	0.013	0.11

TABLE II Solution and step ageing heat treatments (AC = air cooling)

1.	ST	1153 K × 2 h, AC
2.	T1	1143 K × 20 h, AC
3.	T2T1	1223 K × 5 h, AC + 1143 K × 20 h, AC
4.	T3T1	1293 K × 5 h, AC + 1143 K × 20 h, AC
5.	T3T2T1	1293 K × 5 h, AC + 1223 K × 5 h, AC + 1143 K × 20 h, AC

2. Materials and experimental procedures

Two developed nickel-base superalloys (hereafter designated as Alloy B and Alloy C) were prepared by the investment casting process. The compositions are given in Table I and the mechanical properties are presented elsewhere [2, 3]. Both alloys were solution annealed at 1553 K for 2 h and air cooled. Subsequently, they were subjected to step ageing heat treatments as described in Table II. In addition, single geing up to 300 h at 1143, 1223 and 1293 K was also carried out to examine the effects of ageing temperature and ageing time on the growth of γ'.

Specimens were chemically etched in a solution of 10 g CrO_3, 50 ml H_2O and 50 ml HCl. Microstructure was examined in a Hitachi S-4200 scanning electron microscope and in a PHILIPS CM 30 scanning transmission electron microscope. The samples for TEM were ground to a thickness about 60 to 80 μm and then electropolished in a solution containing 10% perchloric acid and 90% methanol at 30 V at temperatures below 240 K. Particle size measurements were made mainly on SEM photographs of the particles. It is realized that quantitative evaluation of microstructural parameters from experimental data may be subject to errors. To minimize the errors introduced by experimental procedures, in this study, more than one hundred particles were measured with great care being taken to maintain identical etching conditions and to obtain a representative distribution of particle size.

The aged specimens were subjected to micro Vickers hardness testing at room temperature. The Vickers hardness was measured in the grain interiors of polished samples using a 200 g load for each ageing time on a ZEISS MHT-4 Microhardness Tester. Owing to the statistical variation in hardness, the average value of the hardness with a deviation of 5 Hv was used.

3. Results and discussion

3.1. Microstructure

The mechanisms involved in the microstructural evolution and the high temperature behaviour of the two developed alloys were found to be similar to some degree. For example, Fig. 1a and b show the typical transmission electron micrographs of Alloy B and Alloy C after solution annealing at 1553 K for 2 h, air cooling followed by ageing at 1223 K for 100 h. The uniform dispersion of fine γ'-precipitates is observed in the matrix grains. These γ–γ' structures are identified from selected area diffraction (SAD) pattern analysis (Fig. 1c). Ricks *et al.* [4] and Yoo *et al.* [5] studied the morphologies of γ'-precipitates in several Ni-base superalloys with different degrees of γ–γ' lattice mismatch and reported that the morphological change of γ'-precipitates during ageing in the sequence of sphere, cube, cubes in a row and dendrite. It should be pointed out that Alloy C exhibited a very sharp cubic γ'-morphology, with the precipitates arranged in relatively aligned rows parallel to [0 0 1] directions, while Alloy B exhibited a small rounded cubic γ'-shape and the precipitate alignment was less pronounced. In the present study the morphology of γ'-precipitates shows

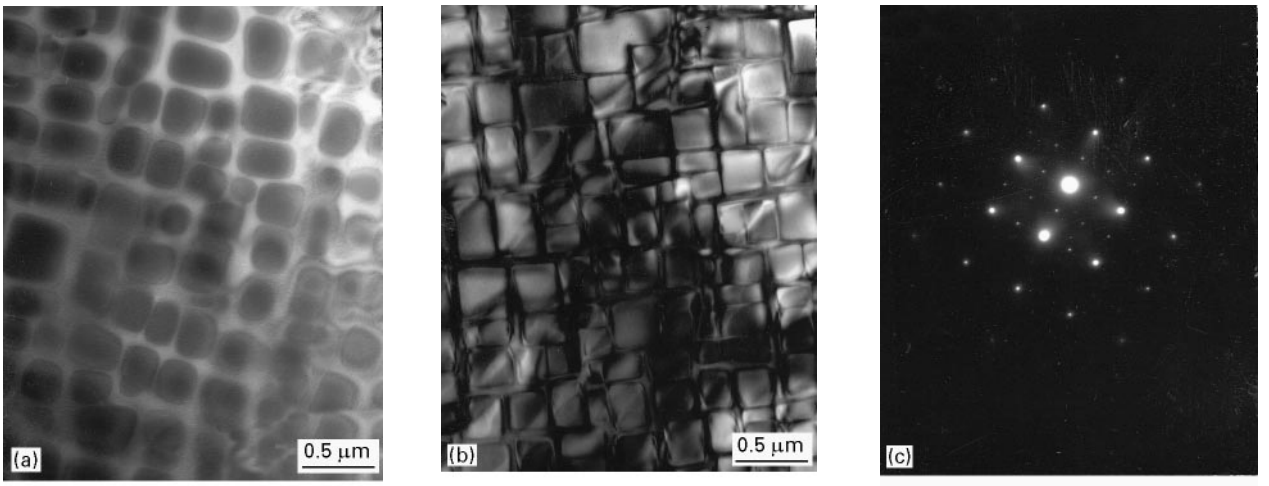

Figure 1 Transmission electron micrographs after solution treatment at 1553 K for 2 h and aged at 1223 K for 100 h for (a) Alloy B, (b) Alloy C, and (c) typical SAD pattern.

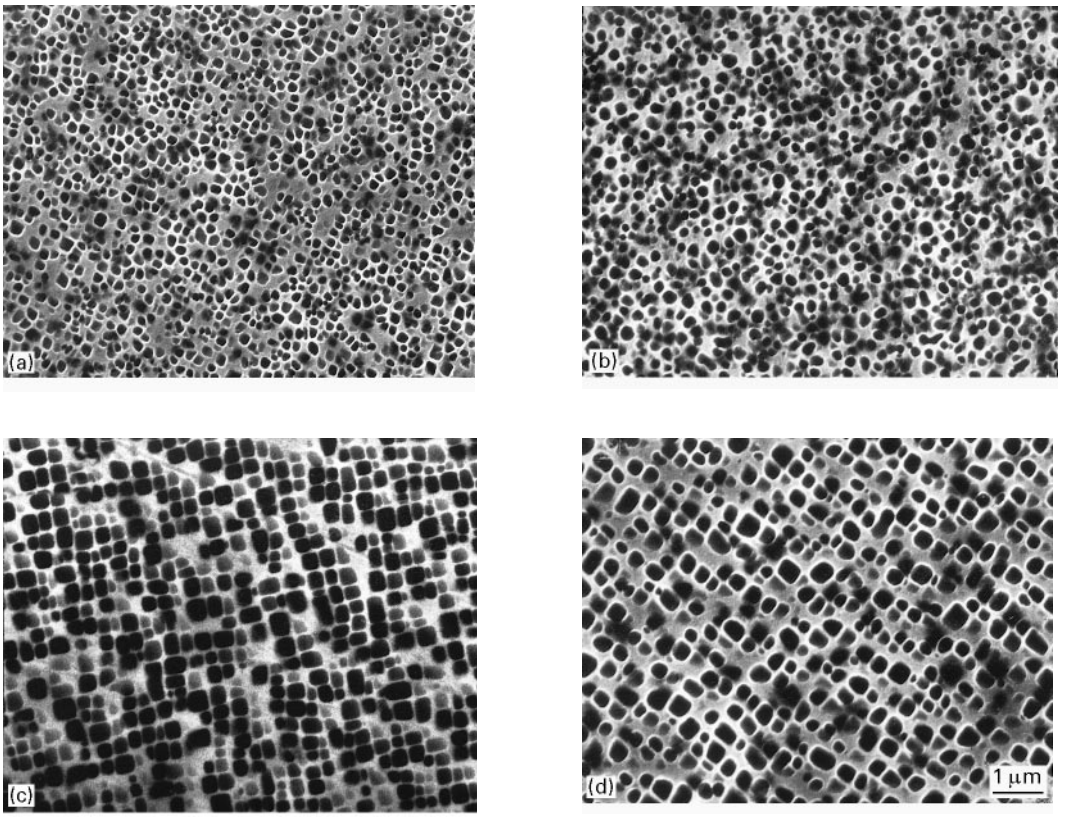

Figure 2 The scanning electron micrographs illustrating the γ–γ′ microstructure of Alloy B aged at (a) T1, (b) T2T1, (c) T3T1 and (d) T3T2T1.

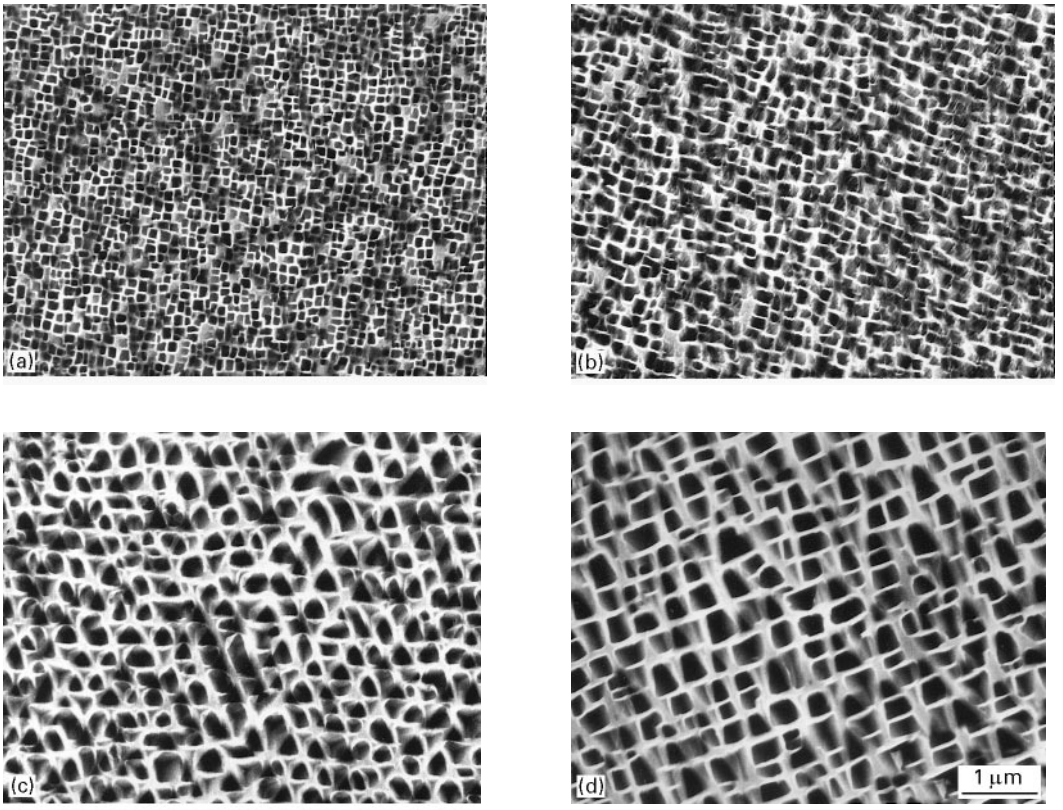

Figure 3 The scanning electron micrographs illustrating the γ–γ′ microstructure of Alloy C aged at (a) T1, (b) T2T1, (c) T3T1 and (d) T3T2T1.

no remarkable change in shape during heat treatment but takes a cubic form.

Figs 2 and 3 show scanning electron micrographs of the specimens of Alloy B and Alloy C at step aged conditions T1, T2T1, T3T1 and T3T2T1. Alloy B exhibited a small rounded cubic γ′-shape at T1 and T2T1 and cubic γ′-shape at T3T1 and T3T2T1, while Alloy C usually exhibited a cubic γ′-morphology. The cubic γ′ is aligned regularly in the developed alloys, which would be beneficial to the mechanical

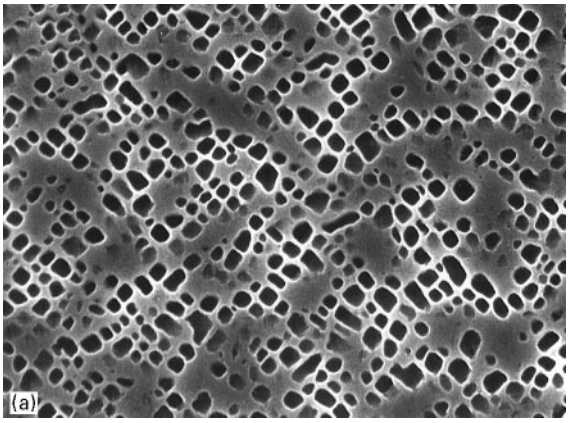

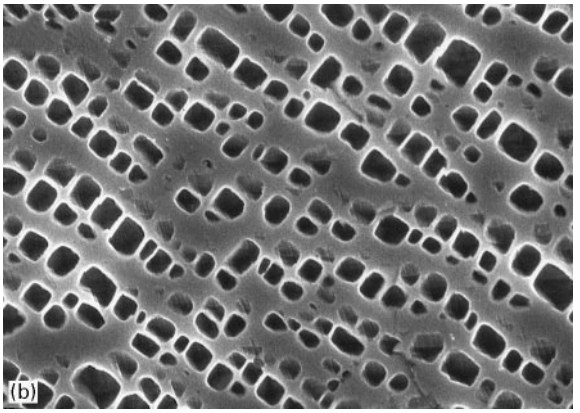

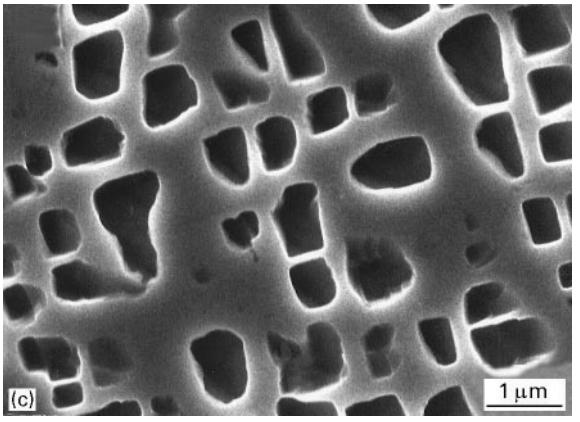

Figure 4 Scanning electron micrographs showing changes in γ'-particle morphology and size in Alloy B aged at 1293 K for (a) 20 h, (b) 100 h and (c) 300 h.

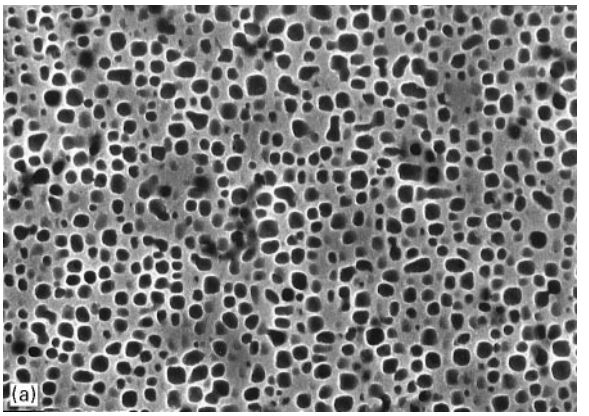

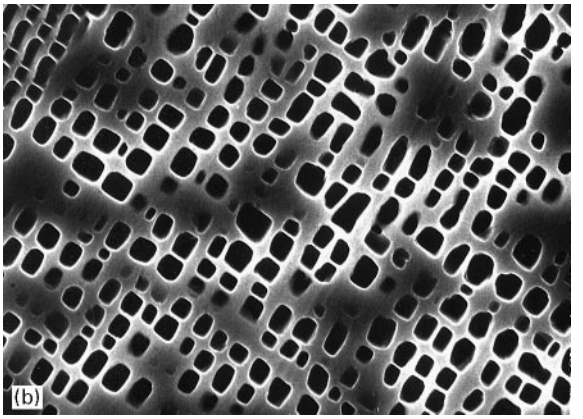

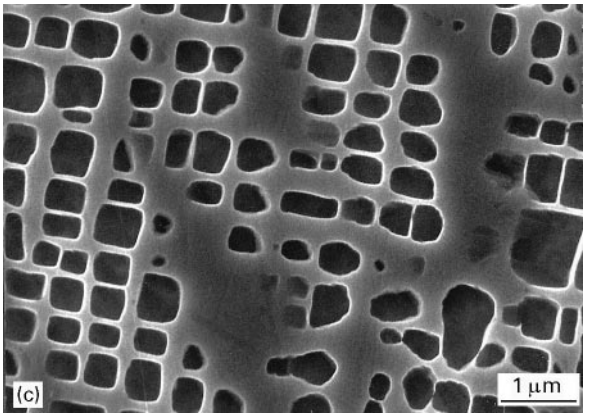

Figure 5 Scanning electron micrographs showing changes in γ'-particle morphology and size in Alloy C aged at 1293 K for (a) 20 h, (b) 100 h and (c) 300 h.

properties [6]. It should be noted that an apparent triangular or multilayer-like cubic γ' can be observed sometimes (Fig. 3c and d) which is probably attributable to incomplete etching and sectioning effects. After prolonged ageing at 1143, 1223 and 1293 K, no TCP precipitation was observed in both of the experiential alloys. Figs 4 and 5 show the changes in γ'-particle morphology and size in Alloy B and Alloy C solution heat treated at 1553 K for 2 h and aged at 1293 K for up to 300 h. It should be noted that the γ'-phase morphologies of designed alloys were also stable compared with those in some reference alloys [7–9]. This result indicates that the mechanical properties of the alloys would not be lowered rapidly by coarsening of the strengthening γ'-phase during high temperature long-term service. This long-term stability is one of the major requirements for the high temperature applications of superalloys.

3.2. Age hardening

Strengthening in superalloys by γ'-particles is related to many factors; the most direct correlation can be made with volume fraction of γ' and with γ'-particle size. However, the correlation between strength and γ'-particle size may be difficult to prove in commercial alloys over the range of particle sizes available. This effect can be demonstrated for tensile or hardness behaviour in low volume fraction γ' alloys, but is not as readily apparent in high volume fraction γ' alloys.

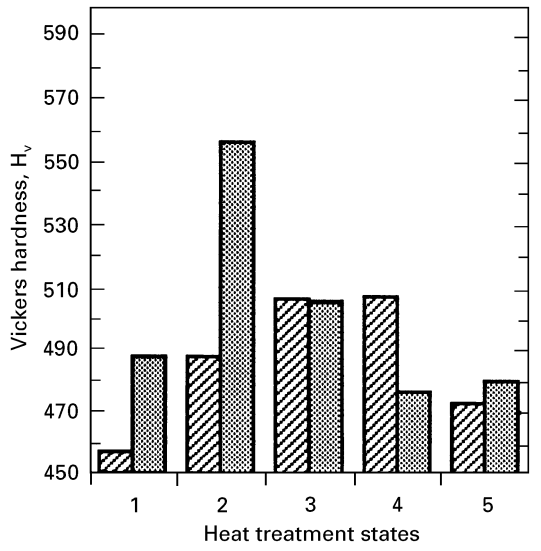

Figure 6 MicroVickers hardness at different step ageing stages. Key: ▨ Alloy B; ▩ Alloy C.

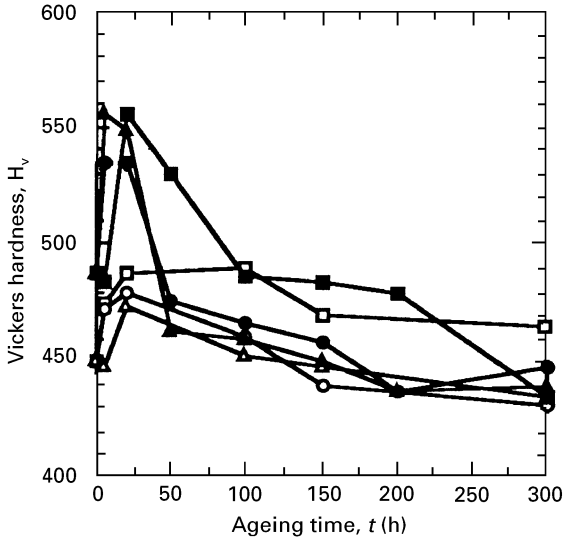

Figure 7 Variation in microVickers hardness with ageing time at various ageing temperatures. Key: –□– 1143 K, Alloy B; –○– 1223 K, Alloy B; –△– 1293 K, Alloy B; –■– 1143 K, Alloy C; –●– 1223 K, Alloy C; –▲–1293 K, Alloy C.

In this study, the γ' strengthening is characterized by hardness testing. Fig. 6 shows the ageing characteristics of Alloy B and Alloy C after step ageing. The age hardening hardly changes in the present alloys, except Alloy C at heat treatment state T1 (1143 K × 20 h). This seems to be a result of high hardness, about 460 Hv and 490 Hv for the as solution treated state for Alloy B and Alloy C, respectively. The hardness increases to 510 Hv after T2T1 (1223 K × 5 h + 1143 K × 20 h) or T3T1 (1293 K × 5 h + 1143 K × 20 h) treatment for Alloy B, while for Alloy C the T1 (1143 K × 20 h) condition proceeds to the highest hardness about 560 Hv. The effects of ageing time and temperature on hardness in Alloy B and Alloy C are shown in Fig. 7. The hardness increases with time to a maximum and softening proceeds after reaching the peak hardness. The time to reach peak hardness is about 60, 25 and 10 h for Alloy B and about 20, 15 and 10 h for Alloy C at 1143, 1223 and 1293 K, respectively. The hardness after 300 h ageing remains high at a value above 430 Hv, which may show that the superior properties can be maintained at high temperatures even after long-term service. This result is consistent with the general tendency in precipitation hardening type alloys.

3.3. Growth of γ'-precipitates

The γ–γ' microstructure of some nickel base superalloys can undergo drastic changes during high temperature heat treatments. The morphology of the γ'-precipitates evolves from different mechanisms: (i) competitive coarsening in order to reduce the specific area of the γ–γ' interface (Ostwald ripening) [10–14] and (ii) shape changes in order to minimize the sum of interfacial and elastic interaction energies. Research works have been conducted concerning the coarsening of the γ'-precipitates during high temperature exposures of the alloys [4, 15–20]. It has been observed that in general the precipitates grow at an almost constant volume fraction, following a $(\text{time})^{1/3}$ power law concerning diffusion-controlled particle coarsening in agreement with the LSW theory of Lifshitz and Slyozov [21] and Wagner [22]. In fact the LSW theory gives the following expressions:

$$r - r_0 = kt^{1/3}$$

$$k = (8\gamma C_e V_m^2 D/9RT)^{1/3}$$

where r is the average particle radius at time t, while r_0 is the same parameter at the onset of the coarsening process; k is the coarsening rate constant, γ is the matrix–particle interface specific free energy, C_e is the matrix concentration of the precipitating elements in equilibrium with a flat surface, V_m is the precipitate molar volume and D is an effective diffusion coefficient mainly depending on the diffusion coefficients of the precipitating elements in the matrix. R and T are the gas constant and the absolute temperature, respectively.

On the assumption that the volume fraction V_f of γ' is independent of the ageing time, the measurements of particle coarsening kinetics were made at 1143, 1223 and 1293 K. γ'-particles in the surface of the specimen can be convex or concave according to the material and etchant. Owing to the distorted cubes of γ'-particles, $(a_1 + a_2)/2$ or $(a_1 a_2)^{1/2}$ is defined as the average cube edge length of a γ'-particle [23], where a_1 and a_2 are two edge lengths of the γ'-particles. Therefore, we obtain $r = \sum(a_1 a_2)^{1/2}/MN$, where r is the average cube length, N the total number of γ'-precipitates measured, and M the magnification of the measured photographs. The particle size data are therefore presented as a plot of $r/2$ versus $kt^{1/3}$ because $r_0/2$ is small and can easily be neglected. The mean sizes of γ'-particles observed in Alloy B and Alloy C with various ageing times at three temperatures are plotted in Fig. 8 as a function of the cube root of ageing time. It is clear that coarsening of γ' in developed alloys obeys the $t^{1/3}$ law, suggesting that the coarsening of γ' in these complex, high volume

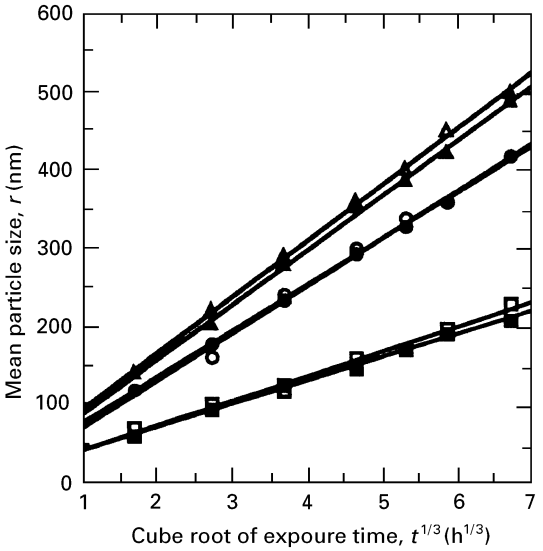

Figure 8 Variation in mean particle size of γ′-precipitates with ageing time at various ageing temperatures. Key: □ 1143 K, Alloy B; ○ 1223 K, Alloy B; △ 1293 K, Alloy B; ■ 1143 K, Alloy C; ●1223 K, Alloy C; ▲ 1293 K, Alloy C.

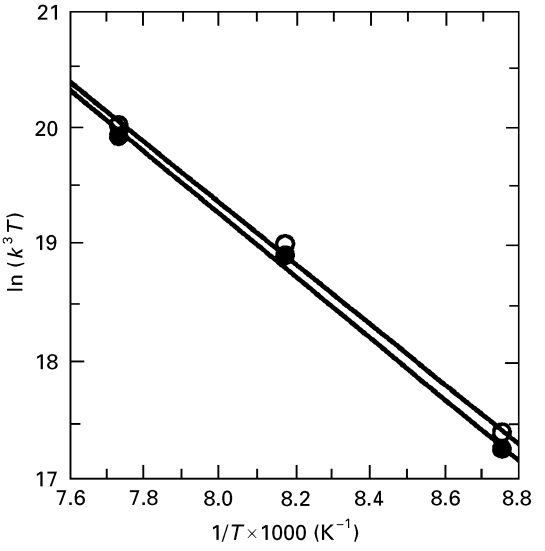

Figure 9 Arrhenius plot for determination of the activation energy for growth of γ′-precipitates. Key: ○ Alloy B, $Q = 272\ kJ\ mol^{-1}$; ●Alloy C, $Q = 277\ kJ\ mol^{-1}$.

fraction superalloys also follows the standard $t^{1/3}$ kinetics of diffusion-controlled particle growth. Similar observations of the cubic growth kinetics of γ′ have also been made in a number of nickel-base superalloys [4, 15–21]. The coarsening rate of γ′-phase in Alloy B is a little larger than that in Alloy C and slower than that in other superalloys [4, 7, 15–21]. The slope of each line in Fig. 8 is a temperature dependent rate constant which can be used to determine the activation energy Q. It is necessary to plot $\ln(k^3T)$ versus T^{-1} as in Fig. 9 to obtain Q values. This yields activation energies of 272 and 277 kJ mol^{-1} for Alloy B and Alloy C. Despite the complexity of these alloys, the activation energies correlate well to that for the volume diffusion of both aluminium and titanium in nickel (270 and 257 kJ mol^{-1} [24], respectively), to the coarsening of γ′ in binary Ni–Al and Ni–Ti alloys (270 [25] and 282 kJ mol^{-1} [26], respectively), and to the coarsening of γ′ in Udinet 700 (270 kJ mol^{-1}) [18]. These results conclusively prove that the growth of γ′ in the alloys is controlled mainly by the volume diffusion of aluminium or titanium in the matrix, although it is also influenced by the interrelated diffusion of other elements away from a growing γ′-particle.

4. Conclusions

Two new cast nickel-base superalloys with superior creep rupture lives at high temperature and high stress were developed in the present study. The age hardening behaviour and microstructural characteristics were studied by microVickers hardness testing and scanning electron and transmission electron microscopy. The growth kinetics of γ′-precipitates were analysed.

The results are summarized as follows:

1. The morphology of γ′ does not change drastically in shape during heat treatments. The γ′ is usually cubic in both Alloy B and Alloy C which is typical morphology present in modern superalloys.

2. Growth of γ′-precipitates proceeds by Ostwald ripening controlled by volume diffusion of solute atoms despite of the high volume fraction of γ′ and complex compositions. The activation energies for the growth are evaluated as 272 and 277 kJ mol^{-1} for Alloy B and Alloy C, respectively.

3. There is no notable changes in hardness after step ageing treatment. During long time ageing, the hardness increases to a peak value at about 20–60 h for Alloy B and at about 10–20 h for Alloy C. Though a softening proceeds after reaching the hardness peak, a high hardness value can still be maintained which may indicate the excellent high temperature properties in the developed alloys.

References

1. N. S. STOLOFF, "Superalloys II" (John Wiley & Sons, New York, 1987) p. 61.
2. X. X. YAO, H. T. KIM and J. CHOI, *Scripta Metall. Mater.* **35** (1996) 953.
3. X. X. YAO, Y. FANG, H. T. KIM and J. CHOI, *Mater. Charact.* **38** (1997) 1.
4. R. A. RICKS, A. J. PORTER and R. C. ECOB, *Acta Metall.* **31** (1983) 43.
5. Y. S. YOO, D. Y. YOON and M. F. HENRY, *Met. Mater.* **1** (1995) 47.
6. R. F. DECKER and C. T. SIMS, "The Superalloys" (John Wiley & Sons, New York, 1972) p. 33.
7. W. S. YANG, *J. Korean Inst. Met. Mater.* **33** (1995) 666.
8. J. S. ZHANG, Z. Q. HU, Y. MURATA, M. MORINAGA and N. YUKAWA, *Metall. Trans.* **24A** (1993) 2443.
9. *Idem, ibid.* **24A** (1993) 2451.
10. A. J. AREDLL, *Acta Metall.* **20** (1972) 61.
11. C. K. L. DAVIES, P. NASH and R. N. STEVENS, *ibid.* **28** (1980) 179.
12. Y. ENEMOTO, M. TOKUYAMA and K. KAWAZAKI, *ibid.* **34** (1986) 2119.
13. D. MACLEAN, *Metal Sci.* **18** (1984) 249.
14. P. K. FOOTNER and B. P. RICHARDS, *J. Mater. Sci.* **17** (1982) 2141.
15. S. B. FISHER and R. J. WHITE, *Mater. Sci. Engng* **33** (1978) 149.

16. P. E. FLEWITT and R. A. STEVENS, *ibid.* **37** (1979) 237.
17. K. B. S. RAO, V. SEETHARAMAN, S. L. MANNAN and P. RODRIGUEZ, *ibid.* **58** (1983) 93.
18. E. H. VAN DER MOLEN, J. M. OBLAK and O. H. KRIEGE, *Metall. Trans.* **2** (1971) 1627.
19. E. NEMBACH, A. S. SCHANZER, W. SCHROER and K. TRINCKAUF, *Acta Metall.* **36** (1988) 1471.
20. K. KUSABIRAKI, X. M. ZHANG and T. OOKA, *ISIJ Int.* **35** (1995) 1115.
21. M. LIFSHITZ and V. V. SLYOZOV, *J. Phys. Chem. Solids* **19** (1961) 35.
22. C. WAGNER, *Z. Electrochem.* **65** (1961) 581.
23. T. L. LIN and M. WEN, *Mater. Sci. Engng* **A113** (1989) 207.
24. R. A. SWALIN and A. MARTIN, *Trans. AIME* **206** (1956) 567.
25. A. J. AREDLL and R. B. NICHOLSON, *Acta Metall.* **14** (1966) 1295.
26. A. J. AREDLL, *Metall. Trans.* **1** (1970) 525.

Received 6 February
and accepted 23 October 1996